*Inorg. Chem.* **2003**, *42*, 8652–8662


# Modeling the Syn Disposition of Nitrogen Donors at the Active Sites of Carboxylate-Bridged Diiron Enzymes. Enforcing Dinuclearity and Kinetic Stability with a 1,2-Diethynylbenzene-Based Ligand

**Jane Kuzelka, Joshua R. Farrell, and Stephen J. Lippard***

*Department of Chemistry, Massachusetts Institute of Technology, Cambridge, Massachusetts 02139*

Received August 4, 2003

The syn coordination of histidine residues at the active sites of several carboxylate-rich non-heme diiron enzymes has been difficult to reproduce with small molecule model compounds. In this study, ligands derived from 1,8-naphthyridine, phthalazine, and 1,2-diethynylbenzene were employed to mimic this geometric feature. The preassembled diiron(II) complex $[Fe_2(\mu\text{-}O_2CAr^{Tol})_2(O_2CAr^{Tol})_2(THF)_2]$ (**1**), where $Ar^{Tol}CO_2^-$ is the sterically hindered carboxylate 2,6-di(*p*-tolyl)benzoate, served as a convenient starting material for the preparation of iron(II) complexes, all of which were crystallographically characterized. Use of the ligand 2,7-dimethyl-1,8-naphthyridine ($Me_2$-napy) afforded the mononuclear complex $[Fe(O_2CAr^{Tol})_2(Me_2\text{-napy})]$ (**2**), whereas dinuclear $[Fe_2(\mu\text{-DMP})(\mu\text{-}O_2CAr^{Tol})_2(O_2CAr^{Tol})_2(THF)]$ (**3**) resulted when 1,4-dimethylphthalazine (DMP) was employed. The dinuclear core of compound **3** is kinetically labile, as evidenced by the formation of $[Fe(O_2CAr^{Tol})_2(vpy)_2]$ (**4**) upon addition of 2-vinylpyridine (vpy). The diiron analogue of **4**, $[Fe_2(\mu\text{-}O_2CAr^{Tol})_2(O_2CAr^{Tol})_2(vpy)_2]$ (**5**), was prepared directly from **1**. When the sterically more demanding ligand 2,6-di(4-*tert*-butylphenyl)benzoate ($Ar^{4\text{-}tBuPh}CO_2^-$) was used, mononuclear $[Fe(O_2CAr^{4\text{-}tBuPh})_2(THF)_2]$ (**6**) and $[Fe(O_2CAr^{4\text{-}tBuPh})_2(DMP)_2]$ (**7**) formed. The difficulty in stabilizing a dinuclear core with these simple $(N)_2$-donor ligands was circumvented by preparing a family of 1,2-diethynylbenzene-based ligands, from which were readily assembled the complexes $[Fe_2(Et_2BCQEB^{Et})(\mu\text{-}O_2CAr^{Tol})_3](OTf)$ (**15**) and $[Cu_2(Et_2BCQEB^{Et})(\mu\text{-}I)_2]$ (**16**), where $Et_2BCQEB^{Et}$ is 1,2-bis(3-ethynyl-8-carboxylatequinoline)benzene ethyl ester. The $Et_2BCQEB^{Et}$ framework provides both structural flexibility and the desired syn nitrogen donor geometry, thus serving as a good first-generation ligand in this class.

## Introduction

Dioxygen-activating metalloenzymes containing carboxylate-bridged diiron centers perform a variety of remarkable chemical reactions. Well-studied members of this class of proteins include the hydroxylase component of soluble methane monooxygenase (sMMOH), an enzyme that converts $CH_4$ into $CH_3OH$,[1−5] the R2 subunit of ribonucleotide reductase (RNR-R2), responsible for the first step of DNA biosynthesis through the generation of a tyrosine radical,[6,7] and Δ-9 desaturase (Δ9D), the diiron core of which effects the desaturation of fatty acids.[8−11] These functions differ dramatically, yet X-ray crystallographic studies reveal strikingly similar active sites.[12−15] As shown in Chart 1, the

* To whom correspondence should be addressed. E-mail: lippard@lippard.mit.edu.

(1) Baik, M.-H.; Newcomb, M.; Friesner, R. A.; Lippard, S. J. *Chem. Rev.* **2003**, *103*, 2385−2419.
(2) Kopp, D. A.; Lippard, S. J. *Curr. Opin. Chem. Biol.* **2002**, *6*, 568−576.
(3) Merkx, M.; Kopp, D. A.; Sazinsky, M. H.; Blazyk, J. L.; Müller, J.; Lippard, S. J. *Angew. Chem., Int. Ed.* **2001**, *40*, 2782−2807.
(4) Lipscomb, J. D.; Lee, S.-K.; Nesheim, J. C.; Jin, Y.; Wallar, B. J.; Zhang, X.-Y. In *Iron Metabolism*; Ferreira, G. C., Moura, J. J. G., Franco, R., Eds.; Wiley-VCH: Weinheim, 1999; pp 323−339.
(5) Lipscomb, J. D.; Que, L., Jr. *J. Biol. Inorg. Chem.* **1998**, *3*, 331−336.
(6) Stubbe, J.; Nocera, D. G.; Yee, C. S.; Chang, M. C. Y. *Chem. Rev.* **2003**, *103*, 2167−2201.
(7) Stubbe, J.; van der Donk, W. A. *Chem. Rev.* **1998**, *98*, 705−762.
(8) Lyle, K. S.; Möenne-Loccoz, P.; Ai, J.; Sanders-Loehr, J.; Loehr, T. M.; Fox, B. G. *Biochemistry* **2000**, *39*, 10507−10513.
(9) Broadwater, J. A.; Achim, C.; Münck, E.; Fox, B. G. *Biochemistry* **1999**, *38*, 12197−12204.
(10) Yang, Y.-S.; Broadwater, J. A.; Pulver, S. C.; Fox, B. G.; Solomon, E. I. *J. Am. Chem. Soc.* **1999**, *121*, 2770−2783.
(11) Shu, L.; Broadwater, J. A.; Achim, C.; Fox, B. G.; Münck, E.; Que, L., Jr. *J. Biol. Inorg. Chem.* **1998**, *3*, 392−400.
(12) Whittington, D. A.; Lippard, S. J. *J. Am. Chem. Soc.* **2001**, *123*, 827−838.
(13) Rosenzweig, A. C.; Frederick, C. A.; Lippard, S. J.; Nordlund, P. *Nature* **1993**, *366*, 537−543.
(14) Logan, D. T.; Su, X.-D.; Åberg, A.; Regnström, K.; Hajdu, J.; Eklund, H.; Nordlund, P. *Structure* **1996**, *4*, 1053−1064.



10.1021/ic034928e CCC: $25.00 
Published on Web 11/22/2003

**Chart 1**

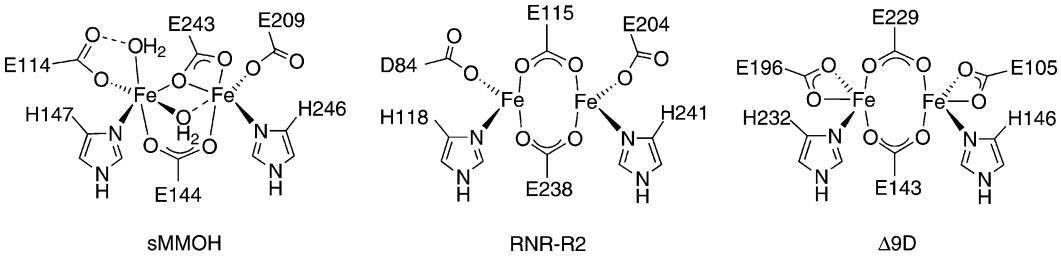


primary coordination spheres of the carboxylate-bridged diiron centers in sMMOH, RNR-R2, and Δ9D comprise four glutamate or aspartate side chains and two histidine residues. Whereas the coordination modes of the carboxylate groups vary among the enzymes, the two nitrogen donors are consistently bound in a syn fashion, on the same side of the Fe···Fe vector. This geometric feature is important both in the activation of dioxygen and subsequent substrate oxidation. For the oxidation of $CH_4$ by sMMOH, which is effected by a di($\mu$-oxo)diiron(IV) species, intermediate Q,[1,16−18] preliminary DFT calculations reveal the conversion to $CH_3OH$ to be energetically unfavorable for histidine residues disposed in the anti geometry.[19]

The ability of carboxylate-bridged diiron units in nature to promote such important chemical transformations has prompted the synthesis of small molecule analogues. The propensity of carboxylate units to form oligomers[20−29] rather than discrete diiron compounds can be overcome with the use of multidentate nitrogen-rich ligands[30] or sterically hindered carboxylate groups.[31,32] The resulting complexes often reproduce features of non-heme metalloproteins including dinuclearity, structural flexibility, and dioxygen-reactivity. All three properties are modeled especially well with the use of the bulky *m*-terphenyl-derived carboxylate ligands displayed in Chart 2. The occurrence of carboxylate shifts in $[Fe_2(O_2CAr')_4(N)_2]$ compounds attests to the flexibility of the building blocks,[31,32] and formation of (peroxo)diiron(III) or di($\mu$-oxo)diiron(III,IV) species mimics the reactive intermediates that form in the catalytic cycles of the related biological systems.[33−37] The activation of strong C−H bonds by these diiron compounds has not yet been achieved, however, possibly because of the invariable anti disposition of the N-donor ligands.

The theoretical prediction that the relative orientation of nitrogen donors may dramatically influence the reactivity of intermediate Q inspired us to investigate its validity with small molecule complexes having this property. Self-assembly methods have thus far failed to produce many such complexes, as manifest by the many compounds with N-donors bound in an anti fashion.[31,32] Our strategy, therefore, was to employ ligands in which the connectivity would enforce the desired coordination mode. We report here the results of our first efforts in this area, in which dimetallic complexes were assembled with several $(N)_2$-ligands employed in conjunction with sterically demanding carboxylate groups. We describe ligands derived from a 1,2-diethynylbenzene backbone and their use in the synthesis of diiron(II)

**Chart 2**

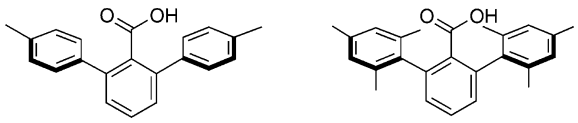



(15) Lindqvist, Y.; Huang, W.; Schneider, G.; Shanklin, J. *EMBO J.* **1996**, *15*, 4081−4092.
(16) Lovell, T.; Himo, F.; Han, W.-G.; Noodleman, L. *Coord. Chem. Rev.* **2003**, *238*−*239*, 211−232.
(17) Siegbahn, P. E. M. *J. Biol. Inorg. Chem.* **2001**, *6*, 27−45.
(18) Shu, L.; Nesheim, J. C.; Kauffmann, K.; Münck, E.; Lipscomb, J. D.; Que, L., Jr. *Science* **1997**, *275*, 515−518.
(19) Baik, M.-H.; Friesner, R. A.; Lippard, S. J. Unpublished results. In a previous DFT study (Baik, M.-H.; Gherman, B. F.; Friesner, R. A.; Lippard, S. J. *J. Am. Chem. Soc.* **2002**, *124*, 14608−14615), the electron-accepting orbital (LUMO) of the reactive intermediate Q was found to be dominated by metal-based orbitals that are aligned in the $Fe_2O_2$ plane. Significant mixing of the N-donor ligand orbitals plays an important role for shaping the LUMO, where the metal−ligand interaction is antibonding as expected for a frontier orbital. The ligand orbitals of the carboxylate groups, on the other hand, do not contribute to the LUMO. This asymmetric antibonding interaction between N and Fe polarizes the metal-based d-orbitals away from the N-donor side of the $Fe_2O_2$ core and increases the LUMO character on the oxo group trans to the N-donor ligands. This atom is therefore more electrophilic, which makes the syn orientation of the N-donor ligands an important structural feature for controlling the reactivity of the $Fe_2O_2$ core. Detailed calculations are continuing and will be reported elsewhere.
(20) Kooijman, H.; Spek, A. L.; Bouwman, E.; Miccichè, F.; Warzeska, S. T.; Reedijk, J. *Acta Crystallogr., Sect. E* **2002**, *58*, m93−m95.
(21) Mandal, S. K.; Young, V. G., Jr.; Que, L., Jr. *Inorg. Chem.* **2000**, *39*, 1831−1833.
(22) Hummel, H.; Bill, E.; Weyhermüller, T.; Wieghardt, K. *Inorg. Chim. Acta* **1999**, *291*, 258−265.
(23) Frey, M.; Harris, S. G.; Holmes, J. M.; Nation, D. A.; Parsons, S.; Tasker, P. A.; Teat, S. J.; Winpenny, R. E. P. *Angew. Chem., Int. Ed.* **1998**, *37*, 3246−3248.
(24) Herold, S.; Lippard, S. J. *Inorg. Chem.* **1997**, *36*, 50−58.
(25) Goldberg, D. P.; Telser, J.; Bastos, C. M.; Lippard, S. J. *Inorg. Chem.* **1995**, *34*, 3011−3024.
(26) Taft, K. L.; Caneschi, A.; Pence, L. E.; Delfs, C. D.; Papaefthymiou, G. C.; Lippard, S. J. *J. Am. Chem. Soc.* **1993**, *115*, 11753−11766.
(27) Taft, K. L.; Papaefthymiou, G. C.; Lippard, S. J. *Science* **1993**, *259*, 1302−1305.
(28) Rardin, R. L.; Poganiuch, P.; Bino, A.; Goldberg, D. P.; Tolman, W. B.; Liu, S.; Lippard, S. J. *J. Am. Chem. Soc.* **1992**, *114*, 5240−5249.
(29) Lippard, S. J. *Angew. Chem., Int. Ed. Engl.* **1988**, *27*, 344−361.
(30) For multidentate ligands derived from pyrazole, naphthyridine, pyridazine, and phthalazine, see references in: Kuzelka, J.; Spingler, B.; Lippard, S. J. *Inorg. Chim. Acta* **2002**, *337*, 212−222.
(31) Lee, D.; Lippard, S. J. *Inorg. Chem.* **2002**, *41*, 2704−2719.
(32) Tolman, W. B.; Que, L., Jr. *J. Chem. Soc., Dalton Trans.* **2002**, 653−660.
(33) Lee, D.; Lippard, S. J. *Inorg. Chem.* **2002**, *41*, 827−837.
(34) Lee, D.; Pierce, B.; Krebs, C.; Hendrich, M. P.; Huynh, B. H.; Lippard, S. J. *J. Am. Chem. Soc.* **2002**, *124*, 3993−4007.
(35) Que, L., Jr.; Tolman, W. B. *Angew. Chem., Int. Ed.* **2002**, *41*, 1114−1137.
(36) Hsu, H.-F.; Dong, Y.; Shu, L.; Young, V. G., Jr.; Que, L., Jr. *J. Am. Chem. Soc.* **1999**, *121*, 5230−5237.
(37) Hagadorn, J. R.; Que, L., Jr.; Tolman, W. B. *J. Am. Chem. Soc.* **1998**, *120*, 13531−13532.

and dicopper(I) compounds. Comparison of the structural features of the resulting complexes reveals that the ligand framework is sufficiently flexible to support features relevant to the formation of intermediate Q of sMMOH.

## Experimental Section

**General Procedures and Methods.** Solvents were saturated with nitrogen and purified by passing over a column of activated $Al_2O_3$ under nitrogen.[38] The compounds $[Fe_2(\mu\text{-}O_2CAr^{Tol})_2(O_2CAr^{Tol})_2(THF)_2]$ (**1**) where $Ar^{Tol}CO_2^-$ is 2,6-di(*p*-tolyl)benzoate,[31] 2,7-dimethyl-1,8-naphthyridine ($Me_2$-napy),[39,40] 1,4-dimethylphthalazine (DMP),[41,42] $Fe(OTf)_2$·2MeCN where OTf is triflate,[43] $NaO_2CAr^{4\text{-}tBuPh}$ where $Ar^{4\text{-}tBuPH}CO_2^-$ is 2,6-di(4-*tert*-butylphenyl-benzoate),[44−47] 8-quinolinecarboxylic acid,[48] 8-quinolinecarboxylate ethyl ester,[48] 3-hydroxy-8-carboxylatequinoline ethyl ester,[49] and 1,2-diiodo-4,5-diethylbenzene[50] were prepared according to published literature procedures. Prior to use, 2-vinylpyridine (vpy) was freshly distilled. All other reagents were purchased from commercial sources and used as received. Air sensitive manipulations were performed by using standard Schlenk techniques or under nitrogen in an MBraun glovebox. NMR spectra were obtained on a 300 MHz Varian Unity or Mercury spectrometer, and melting points were determined with a Thomas-Hoover capillary melting point apparatus. ESI-MS spectra were recorded on a Bruker Daltonics APEXII 3 T Fourier transform mass spectrometer in the MIT Department of Chemistry Instrumentation Facility. FT-IR data for compounds **2**−**16** are provided in the Supporting Information.

**$[Fe(O_2CAr^{Tol})_2(Me_2\text{-napy})]$ (2).** Treatment of **1** (60 mg, 0.041 mmol) in $CH_2Cl_2$ (2 mL) with $Me_2$-napy (14.3 mg, 0.0905 mmol) in $CH_2Cl_2$ (1 mL) afforded a pink-red solution that was stirred for 15 min. The solution was filtered through Celite, and to the filtrate was added THF (1 mL). Vapor diffusion of $Et_2O$ into this solution yielded **2** as pink prisms that were suitable for X-ray diffraction study (54 mg, 81%). Anal. Calcd for $C_{52}H_{44}N_2O_4Fe$: C, 76.47; H, 5.43; N, 3.43. Found: C, 76.65; H, 5.70; N, 3.70.

**$[Fe_2(\mu\text{-DMP})(\mu\text{-}O_2CAr^{Tol})_2(O_2CAr^{Tol})_2(THF)]$ (3).** To a clear solution of **1** (200 mg, 0.137 mmol) in $CH_2Cl_2$ (2 mL) was added DMP (24 mg, 0.15 mmol) in $CH_2Cl_2$ (1 mL), and the color turned orange. The reaction mixture was stirred for 15 min and filtered through Celite. Addition of THF (1 mL) and exposure to pentane vapor diffusion yielded yellow-orange needles of **3** (204 mg, 94%). Anal. Calcd for $C_{98}H_{86}N_2O_9Fe_2$: C, 76.07; H, 5.60; N, 1.81. Found: C, 76.03; H, 5.51; N, 1.93.

**$[Fe(O_2CAr^{Tol})_2(vpy)_2]$ (4).** Treatment of **3** (61 mg, 0.039 mmol) in $CH_2Cl_2$ (2 mL) with vpy (84 $\mu$L, 0.78 mmol) afforded an orange solution that was stirred for 30 min. Volatile components were evaporated under reduced pressure, and the residue was redissolved in $CH_2Cl_2$. Exposure of this solution to $Et_2O$ vapor diffusion yielded orange crystals of **4** that were suitable for X-ray diffraction (53 mg, 78%). Anal. Calcd for $C_{56}H_{48}N_2O_4Fe$: C, 77.41; H, 5.57; N, 3.22. Found: C, 77.22; H, 5.60; N, 3.12.

**$[Fe_2(\mu\text{-}O_2CAr^{Tol})_2(O_2CAr^{Tol})_2(vpy)_2]$ (5).** To **1** (100 mg, 0.0685 mmol) in $CH_2Cl_2$ (2 mL) was added vpy (14.8 $\mu$L, 0.137 mmol), and the resulting bright yellow solution was stirred for 15 min. The solvent was removed under reduced pressure, and recrystallization of the residue from $CH_2Cl_2$ by $Et_2O$ vapor diffusion yielded **5**·$2CH_2Cl_2$·MeOH as yellow crystals of X-ray diffraction quality (88 mg, 85%). Anal. Calcd for $C_{98}H_{82}N_2O_8Fe_2$: C, 77.06; H, 5.41; N, 1.83. Found: C, 76.59; H, 5.83; N, 1.54.

**$[Fe(O_2CAr^{4\text{-}tBuPh})_2(THF)_2]$ (6).** To $Fe(OTf)_2$·2MeCN (214 mg, 0.491 mmol) in THF (8 mL) was added solid $NaO_2CAr^{4\text{-}tBuPh}$ (400 mg, 0.980 mmol), and the pale yellow solution was stirred for 30 min. The solvent was evaporated under reduced pressure, and to the residue was added $CH_2Cl_2$. The resulting suspension was filtered through a medium-porosity frit, and the filtrate was evaporated to dryness under reduced pressure. The off-white solid was recrystallized from THF by pentane vapor diffusion to yield colorless crystals of **6** that were suitable for X-ray diffraction study (309 mg, 65%). Anal. Calcd for $C_{62}H_{74}O_6Fe$: C, 76.68; H, 7.68. Found: C, 76.38; H, 7.65.

**$[Fe(O_2CAr^{4\text{-}tBuPh})_2(DMP)_2]$ (7).** Treatment of **6** (100 mg, 0.104 mmol) in $CH_2Cl_2$ (3 mL) with DMP (33 mg, 0.21 mmol) in $CH_2Cl_2$ (1 mL) rapidly generated an orange solution that was stirred for 30 min. The reaction mixture was filtered through Celite, and THF (1 mL) was added. Exposure of this solution to $Et_2O$ vapor diffusion afforded orange X-ray quality crystals of **7**·2THF (80 mg, 68%). Anal. Calcd for $C_{74}H_{78}N_4O_4Fe$: C, 77.74; H, 6.88; N, 4.90. Found: C, 77.81; H, 6.73; N, 4.79.

**3-Trifluoromethanesulfonate-8-carboxylatequinoline Ethyl Ester (8).** An oven-dried 200 mL three-neck round-bottom flask was cooled to room temperature under $N_2$ and charged with 3-hydroxy-8-quinolinecarboxylate ethyl ester (4.42 g, 20.4 mmol), freshly distilled $CH_2Cl_2$ (80 mL), and dry pyridine (15 mL). The resulting pale orange solution was further cooled to 0 °C in an ice−water bath, and triflic anhydride (3.43 mL, 20.4 mmol) was slowly added via syringe. The orange solution was warmed to room temperature over ∼5 h and washed with saturated aqueous $NaHCO_3$ (100 mL), and the product was extracted with $CH_2Cl_2$ (3 × 50 mL). The organic layer was dried over $MgSO_4$ and filtered, and the solvent was removed by rotary evaporation. The resulting pink-orange solid **8** (6.73 g, 95%) was used in subsequent reactions with no additional purification. ESI-MS (+*m*/*z*) Calcd for $(M + Na)^+$: 372.0130. Found: 372.0113. $^1$H NMR (300 MHz, $CDCl_3$): $\delta$ 8.96 d ($J$ = 9 Hz, 1H), 8.13−8.09 m (2H), 8.01 dd (1H), 7.72−7.67 m (1H), 4.54 q ($J$ = 24 Hz, 2H), 1.47 t ($J$ = 23 Hz, 3H). $^{13}$C NMR (75 MHz, $CDCl_3$): $\delta$ 166.92, 144.61, 144.26, 143.45, 132.36, 131.34, 131.22, 128.01, 127.69, 127.16, 118.79 q, 62.02, 14.59. $^{19}$F NMR (282 MHz, $CDCl_3$): $\delta$ 103.41. Mp 87−90 °C.

**3-Trimethylsilanylethynyl-8-carboxylatequinoline Ethyl Ester (9).** A 20 mL scintillation vial was charged with **8** (1.0 g, 2.9 mmol) and THF (15 mL) under a $N_2$ atmosphere. To the resulting mixture was added $[PdCl_2(PPh_3)_2]$ (98 mg, 0.14 mmol), $PPh_3$ (19 mg, 0.072 mmol), $NEt_3$ (599.3 $\mu$L, 4.308 mmol), and $HCCSiMe_3$ (606.3 $\mu$L, 4.386 mmol). The dark red suspension was stirred for 15 min, after which time CuI (6.5 mg, 0.034 mmol) was added and the mixture was stirred vigorously overnight. Rotary evaporation of the volatile components afforded a dark red oil that was dissolved in $CH_2Cl_2$ and purified by column chromatography on silica gel (3:1 hexanes/EtOAc). The resulting pale yellow oil was triturated to yield **9** as


(38) Pangborn, A. B.; Giardello, M. A.; Grubbs, R. H.; Rosen, R. K.; Timmers, F. J. *Organometallics* **1996**, *15*, 1518−1520.
(39) He, C.; Lippard, S. J. *Tetrahedron* **2000**, *56*, 8245−8252.
(40) Chandler, C. J.; Deady, L. W.; Reiss, J. A.; Tzimos, V. *J. Heterocycl. Chem.* **1982**, *19*, 1017−1019.
(41) Guyot, A.; Vallette, F. *Ann. Chim. (Paris)* **1911**, *23*, 390−391.
(42) Guyot, A.; Catel, J. *Bull. Soc. Chim. Fr.* **1906**, *35*, 1139−1140.
(43) Hagen, K. S. *Inorg. Chem.* **2000**, *39*, 5867−5869.
(44) Lee, D.; Sorace, L.; Caneschi, A.; Lippard, S. J. *Inorg. Chem.* **2001**, *40*, 6774−6781.
(45) Saednya, A.; Hart, H. *Synthesis* **1996**, 1455−1458.
(46) Chen, C.-T.; Siegel, J. S. *J. Am. Chem. Soc.* **1994**, *116*, 5959−5960.
(47) Du, C.-J. F.; Hart, H.; Ng, K.-K. D. *J. Org. Chem.* **1986**, *51*, 3162−3165.
(48) Campbell, K. N.; Kerwin, J. F.; LaForge, R. A.; Campbell, B. K. *J. Am. Chem. Soc.* **1946**, *68*, 1844−1846.
(49) Ochiai, E.; Kaneko, C.; Shimada, I.; Murata, Y.; Kosuge, T.; Miyashita, S.; Kawasaki, C. *Chem. Pharm. Bull.* **1960**, *8*, 126−130.
(50) Zhou, Q.; Carroll, P. J.; Swager, T. M. *J. Org. Chem.* **1994**, *59*, 1294−1301.

a light yellow solid (0.7 g, 82%). ESI-MS (+*m*/*z*) Calcd for $(M + Na)^+$: 320.1083. Found: 320.1066. $^1$H NMR (300 MHz, $CDCl_3$): $\delta$ 9.03 d ($J$ = 7 Hz, 1H), 8.28 d ($J$ = 7 Hz, 1H), 8.03 dd (1H), 7.89 dd (1H), 7.59 m (1H), 4.54 q ($J$ = 23 Hz, 2H), 1.46 t ($J$ = 23 Hz, 3H), 0.31 s (9H). $^{13}$C NMR (75 MHz, $CDCl_3$): $\delta$ 167.31, 153.15, 144.04, 138.90, 131.86, 130.88, 130.77, 127.25, 126.33, 117.93, 101.67, 99.05, 61.73, 14.60, 0.15. Mp 54−57 °C.

**3-Ethynyl-8-carboxylatequinoline Ethyl Ester (10).** To a solution of **9** (1.02 g, 3.43 mmol) in THF (80 mL) was added a 1 M solution of $Bu_4NF$ in THF (3.43 mL, 3.43 mmol), and the resulting dark red solution was stirred for 2 h under $N_2$. The solvent was removed under reduced pressure, and the resulting dark red oil was dissolved in $CH_2Cl_2$ and purified by column chromatography on silica gel (1:1 EtOAc/hexanes). Compound **10** was isolated as a cream-colored solid (0.39 g, 51%). ESI-MS (+*m*/*z*) Calcd for $(M + Na)^+$: 248.0688. Found: 248.0680. $^1$H NMR (300 MHz, $CDCl_3$): $\delta$ 9.02 d ($J$ = 7 Hz, 1H), 8.32 d ($J$ = 6 Hz, 1H), 8.05 dd (1H), 7.92 dd (1H), 7.61 m (1H), 4.56 q ($J$ = 24 Hz, 2H), 3.33 s (1H), 1.48 t ($J$ = 24 Hz, 3H). $^{13}$C NMR (75 MHz, $CDCl_3$): $\delta$ 167.27, 153.17, 144.29, 139.34, 131.95, 131.02, 130.92, 127.19, 126.49, 116.92, 81.35, 80.65, 61.82, 14.63. Mp 90−93 °C.

**1,2-Bis(3-ethynyl-8-carboxylatequinoline)benzene Ethyl Ester ($Et_2$BCQEB, 11).** A thick-walled reaction tube was charged with 1,2-diiodobenzene (79.3 $\mu$L, 0.61 mmol), **10** (0.30 g, 1.3 mmol), $[PdCl_2(PPh_3)_2]$ (43 mg, 0.061 mmol), $PPh_3$ (7.8 mg, 0.030 mmol), CuI (2.7 mg, 0.014 mmol), and $Et_2NH$ (10 mL). The reaction vessel was sealed under $N_2$ with a screw-top lid, and the mixture was heated at 70 °C overnight behind a blast shield. Rotary evaporation of the solvent yielded a dark red oil that was dissolved in $CH_2Cl_2$ and purified by column chromatography on silica gel (1:1 EtOAc/hexanes). The resulting oily orange residue was dissolved in hot MeOH and placed in a −20 °C freezer overnight. Compound **11** was collected as an off-white solid (211 mg, 66%) and washed with cold MeOH. ESI-MS (+*m*/*z*) Calcd for $(M + Na)^+$: 547.1634. Found: 547.1608. $^1$H NMR (300 MHz, $CDCl_3$): $\delta$ 9.13 d ($J$ = 7 Hz, 2H), 8.31 d ($J$ = 7 Hz, 2H), 8.00 dd (2H), 7.83 dd (2H), 7.63 m (2H), 7.54 m (2H), 7.37 m (2H), 4.52 q ($J$ = 23 Hz 4H), 1.44 t ($J$ = 23 Hz, 6 H). $^{13}$C NMR (75 MHz, $CDCl_3$): $\delta$ 167.43, 152.87, 144.22, 138.48, 132.34, 132.06, 131.05, 130.91, 128.89, 127.47, 126.55, 125.20, 117.95, 91.87, 90.73, 61.86, 14.68. Mp 91−93 °C.

**1,2-Bis(3-ethynyl-8-carboxylatequinoline)benzene, Potassium Salt ($K_2$BCQEB, 12).** To **11** (100 mg, 0.190 mmol) in THF (6 mL) was added $KOSiMe_3$ (54 mg, 0.42 mmol) in THF (5 mL) under $N_2$, and the resulting suspension was stirred overnight. The off-white solid **12** was collected and washed with $Et_2O$ (100 mg, 97%). ESI-MS (-*m*/*z*) Calcd for $(M - K)^-$: 505.0591. Found: 505.0575. $^1$H NMR (300 MHz, $CD_3OD$): $\delta$ 9.02 d ($J$ = 7 Hz, 2H), 8.49 d ($J$ = 7 Hz, 2H), 7.79 m (4H), 7.69 m (2H), 7.58 m (2H), 7.46 m (2H). Mp > 300 °C.

**1,2-Bis(3-ethynyl-8-carboxylatequinoline)-4,5-diethylbenzene Ethyl Ester ($Et_2$BCQEB$^{Et}$, 13).** This compound was prepared in a procedure analogous to that used for the synthesis of **11** by substituting 1,2-diiodo-4,5-diethylbenzene for 1,2-diiodobenzene. Purification was achieved by column chromatography on silica gel (1:1 EtOAc/hexanes) followed by recrystallization from EtOH to yield **13** as an off-white solid (45%). ESI-MS (+*m*/*z*) Calcd for $(M + Na)^+$: 603.2260. Found: 603.2255. $^1$H NMR (300 MHz, $CDCl_3$): $\delta$ 9.19 d ($J$ = 8 Hz, 2H), 8.36 d ($J$ = 7 Hz 2H), 8.05 dd (2H), 7.90 dd (2H), 7.60 m (2H), 7.49 s (2H), 4.56 q ($J$ = 24 Hz, 4H), 2.74 q ($J$ = 26 Hz, 4H), 1.48 t ($J$ = 24 Hz, 6H), 1.32 t ($J$ = 26 Hz, 6H). $^{13}$C NMR (75 MHz, $CDCl_3$): $\delta$ 167.46, 152.97, 144.06, 143.38, 138.38, 132.11, 131.99, 131.06, 130.85, 127.59, 126.54, 122.62, 118.33, 92.45, 89.69, 61.88, 25.67, 15.15, 14.70. Mp 125−127 °C.

**1,2-Bis(3-ethynyl-8-carboxylatequinoline)-4,5-diethylbenzene, Sodium Salt ($Na_2$BCQEB$^{Et}$, 14).** A suspension of **13** (85 mg, 0.15 mmol) in MeOH (15 mL) was refluxed for 1 h, at which time the resulting pale yellow solution was treated with an aqueous solution of NaOH (1 M, 0.31 $\mu$L, 0.31 mmol). The mixture was refluxed overnight, and the solvent was removed under reduced pressure to afford **14** as a tan powder in quantitative yield. ESI-MS (−*m*/*z*) Calcd for $(M - 2Na + H)^-$: 523.1658. Found: 523.1651. $^1$H NMR (300 MHz, $CD_3OD$): $\delta$ 9.02 m (2H), 8.46 m (2H), 7.80 m (4H), 7.58 m (2H), 7.50 s (2H), 2.75 q ($J$ = 20 Hz, 4H), 1.30 t ($J$ = 26 Hz, 6H). Mp > 300 °C.

**$[Fe_2(Et_2BCQEB^{Et})(\mu\text{-}O_2CAr^{Tol})_3](OTf)$ (15).** A mixture of $Fe(OTf)_2 \cdot 2MeCN$ (60 mg, 0.14 mmol) in THF (3 mL) was treated with a solution of **13** (40 mg, 0.069 mmol) in THF (2 mL). To the resulting bright orange solution was added solid $NaO_2CAr^{Tol}$ (67 mg, 0.21 mmol), and the suspension was stirred for 2 h. The solvent was evaporated under reduced pressure, and the residue was dissolved in $CH_2Cl_2$ and filtered through a plug of Celite. Pink-red crystals of **15**$\cdot 3.25CH_2Cl_2 \cdot Et_2O$, suitable for X-ray crystallographic study, were obtained from a saturated solution of $CH_2Cl_2$ and $Et_2O$ at room temperature (50 mg, 42%). Anal. Calcd for $C_{102}H_{83}N_2O_{13}F_3SFe_2$: C, 70.19; H, 4.79; N, 1.60. Found: C, 69.98; H, 4.88; N, 1.61.

**$[Cu_2(Et_2BCQEB^{Et})(\mu\text{-}I)_2]$ (16).** To **13** (50 mg, 0.086 mmol) in $CH_2Cl_2$ (2 mL) was added CuI (33 mg, 0.17 mmol) in $Et_2NH$ (2 mL), and the pale yellow solution was stirred for 30 min. The solvent was evaporated under reduced pressure, and the residue was dissolved in $CH_2Cl_2$ to afford an orange solution. Exposure of this solution to $Et_2O$ vapor diffusion afforded **16** as a flocculent orange solid (57 mg, 69%), and single crystals of **16**$\cdot CH_2Cl_2$, suitable for X-ray diffraction study, were obtained by slow $Et_2O$ vapor diffusion. Anal. Calcd for $C_{38}H_{32}N_2O_4I_2Cu_2$: C, 47.47; H, 3.35; N, 2.91. Found: C, 47.25; H, 3.31; N, 2.89.

**X-ray Crystallographic Studies.** Crystals were mounted in Paratone N oil on the ends of glass capillaries and frozen into place under a low-temperature nitrogen cold stream. Data were collected on a Bruker (formerly Siemens) APEX CCD X-ray diffractometer running the SMART software package,[51] with Mo K$\alpha$ radiation ($\lambda$ = 0.71073 Å), and refined using SAINT software.[52] Details of the data collection and reduction protocols are discussed in detail elsewhere.[53] The structures were solved by direct methods using SHELXS-97 software[54] and refined on $F^2$ by using the SHELXL-97 program[55] incorporated in the SHELXTL software package.[56] The program SADABS was used to apply empirical absorption corrections,[57] and PLATON was used to check the possibility of higher symmetry.[58] All non-hydrogen atoms were located and their positions refined with anisotropic thermal parameters by least-

(51) *SMART v5.626: Software for the CCD Detector System*; Bruker AXS: Madison, WI, 2000.
(52) *SAINT v5.01: Software for the CCD Detector System*; Bruker AXS: Madison, WI, 1998.
(53) Feig, A. L.; Bautista, M. T.; Lippard, S. J. *Inorg. Chem.* **1996**, *35*, 6892−6898.
(54) Sheldrick, G. M. *SHELXS-97: Program for the Solution of Crystal Structure*; University of Göttingen: Göttingen, Germany, 1997.
(55) Sheldrick, G. M. *SHELXL-97: Program for the Solution of Crystal Structure*; University of Göttingen: Göttingen, Germany, 1997.
(56) *SHELXTL v5.10: Program Library for Structure Solution and Molecular Graphics*; Bruker AXS: Madison, WI, 1998.
(57) Sheldrick, G. M. *SADABS: Area-Detector Absorption Correction*; University of Göttingen: Göttingen, Germany, 1996.
(58) Spek, A. L. *PLATON, A Multipurpose Crystallographic Tool*; Utrecht University: Utrecht, The Netherlands, 2000.

**Scheme 1**

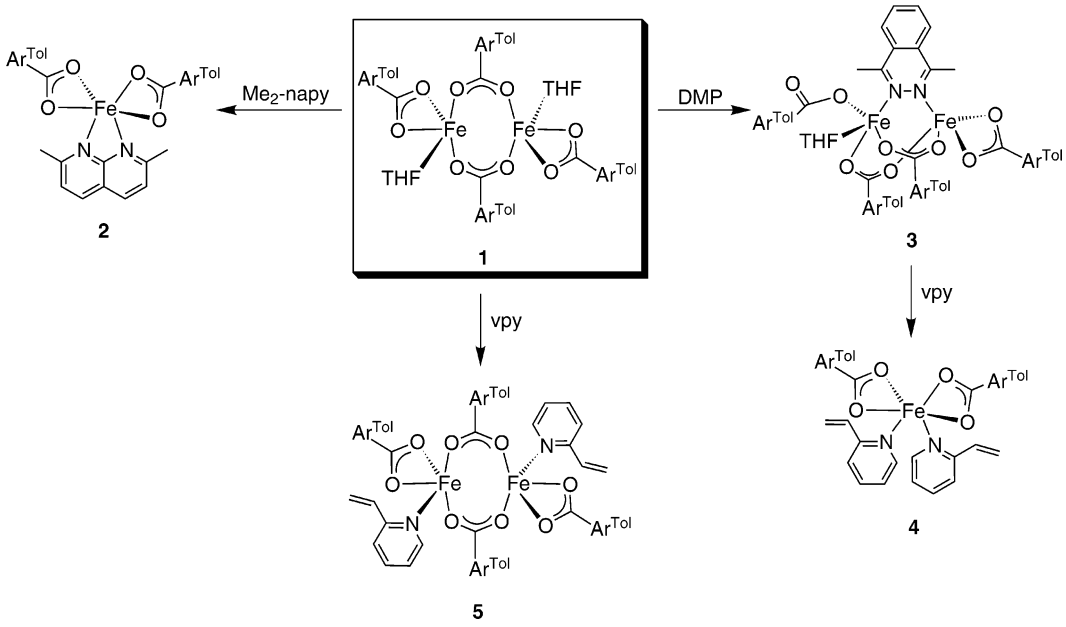


squares cycles and Fourier syntheses. Hydrogen atoms were assigned idealized positions and given a thermal parameter 1.2 times that of the carbon atom to which each was attached.

The crystallographically equivalent dichloromethane solvent molecules in the structure of **5** have one chlorine atom that was disordered over two positions and refined with occupancies of 50%. In addition, there are two half-occupied methanol solvent molecules. In the structure of **6**, the methyl groups of one *tert*-butyl substituent of the crystallographically equivalent $Ar^{4\text{-}tBuPh}CO_2^-$ ligands were disordered over two positions and refined with occupancies of 81% and 19%. In the structure of **15**, one ethyl group of the $Et_2BCQEB^{Et}$ backbone is disordered over two positions and was refined with occupancies of 75% and 25%, and the sulfur atom of the triflate counterion was modeled over two positions with occupancies of 82% and 18%. Five dichloromethane solvent molecules were found in the structure of **15**. One chlorine atom in two molecules was disordered over two positions and modeled with occupancies of 50/50% and 75/25%, respectively. Two additional molecules were refined with 50% occupancy, and one chlorine molecule of each was shared by another dichloromethane molecule, the occupancy of which was refined as 25%. In the refinement of **16**, high angle reflections were omitted to remove high residual electron density located near the iodine atoms resulting from an incomplete absorption correction. Because several carbon atoms of the $Et_2BCQEB^{Et}$ ligand refined as nonpositive definite, only the heteroatoms and the dichloromethane solvent molecule were assigned anisotropic thermal parameters. Details of this structure are provided in Supporting Information. The structures of **2**, **4**−**7**, and **15** are shown in Figures 1 and 3, crystallographic data are listed in Table 1, and selected bond lengths and angles are provided in Tables 2 and 3.

## Results

**A Simple Naphthyridine Ligand: Synthesis and Structural Characterization of $[Fe(O_2CAr^{Tol})_2(Me_2\text{-napy})]$ (2).** Our laboratory has previously employed multidentate 1,8-naphthyridine-based ligands to prepare a variety of diiron(II) compounds.[59−61] In search for a unit that would provide two nitrogen donors for coordination to the diiron core in a syn fashion, we reasoned that a simple naphthyridine derivative might, by virtue of its connectivity, be a suitable candidate. We employed as starting material $[Fe_2(\mu\text{-}O_2CAr^{Tol})_2(O_2CAr^{Tol})_2(THF)_2]$ (**1**), a complex with a preassembled, carboxylate-rich diiron(II) core and two readily displaceable THF molecules (Scheme 1).[31] Reaction of **1** with $Me_2$-napy in a ratio of 1:1 afforded the mononuclear complex **2**, the yield of which was subsequently optimized (>80%) by use of 2 equiv of $Me_2$-napy. Disruption of the dinuclear cores of **1** and the related compound $[Fe_2(\mu\text{-}O_2CAr^{Mes})_2(O_2CAr^{Mes})_2(MeCN)_2]$ has similarly been observed by addition of basic N-donor ligands.[37,62,63]

The structure of **2** reveals that the two nitrogen atoms of $Me_2$-napy chelate a single highly distorted octahedral metal ion (Figure 1, Table 2). The N−Fe−N bite angle of 60.93(9)° is within the range reported for other transition-metal complexes coordinated by bidentate 1,8-naphthyridine fragments,[64−68] and this small angle is responsible for the pronounced distortion at the metal center. The two $Ar^{Tol}CO_2^-$ ligands are bound quite symmetrically to the iron(II) ion in an $\eta^2$-fashion, with Fe−O bond lengths of 2.137(2) and 2.180(2) Å. Similar structures result with other N-donors and sterically demanding *m*-terphenyl-derived carboxylate ligands,[62,63] but not with simpler carboxylates such as acetate

(59) Kuzelka, J.; Mukhopadhyay, S.; Spingler, B.; Lippard, S. J. *Inorg. Chem.* **2003**, *42*, 6447−6457.
(60) He, C.; Lippard, S. J. *Inorg. Chem.* **2001**, *40*, 1414−1420.
(61) He, C.; Barrios, A. M.; Lee, D.; Kuzelka, J.; Davydov, R. M.; Lippard, S. J. *J. Am. Chem. Soc.* **2000**, *122*, 12683−12690.
(62) Lee, D.; Lippard, S. J. *Inorg. Chim. Acta* **2002**, *341*, 1−11.
(63) Hagadorn, J. R.; Que, L., Jr.; Tolman, W. B. *Inorg. Chem.* **2000**, *39*, 6086−6090.
(64) Nakajima, H.; Nagao, H.; Tanaka, K. *J. Chem. Soc., Dalton Trans.* **1996**, 1405−1409.
(65) Bermejo, M.-J.; Ruiz, J.-I.; Solans, X.; Vinaixa, J. *J. Organomet. Chem.* **1993**, *463*, 143−150.
(66) Dewan, J. C.; Kepert, D. L.; White, A. H. *J. Chem. Soc., Dalton Trans.* **1975**, 490−492.
(67) Epstein, J. M.; Dewan, J. C.; Kepert, D. L.; White, A. H. *J. Chem. Soc., Dalton Trans.* **1974**, 1949−1954.
(68) Singh, P.; Clearfield, A.; Bernal, I. *J. Coord. Chem.* **1971**, *1*, 29−37.

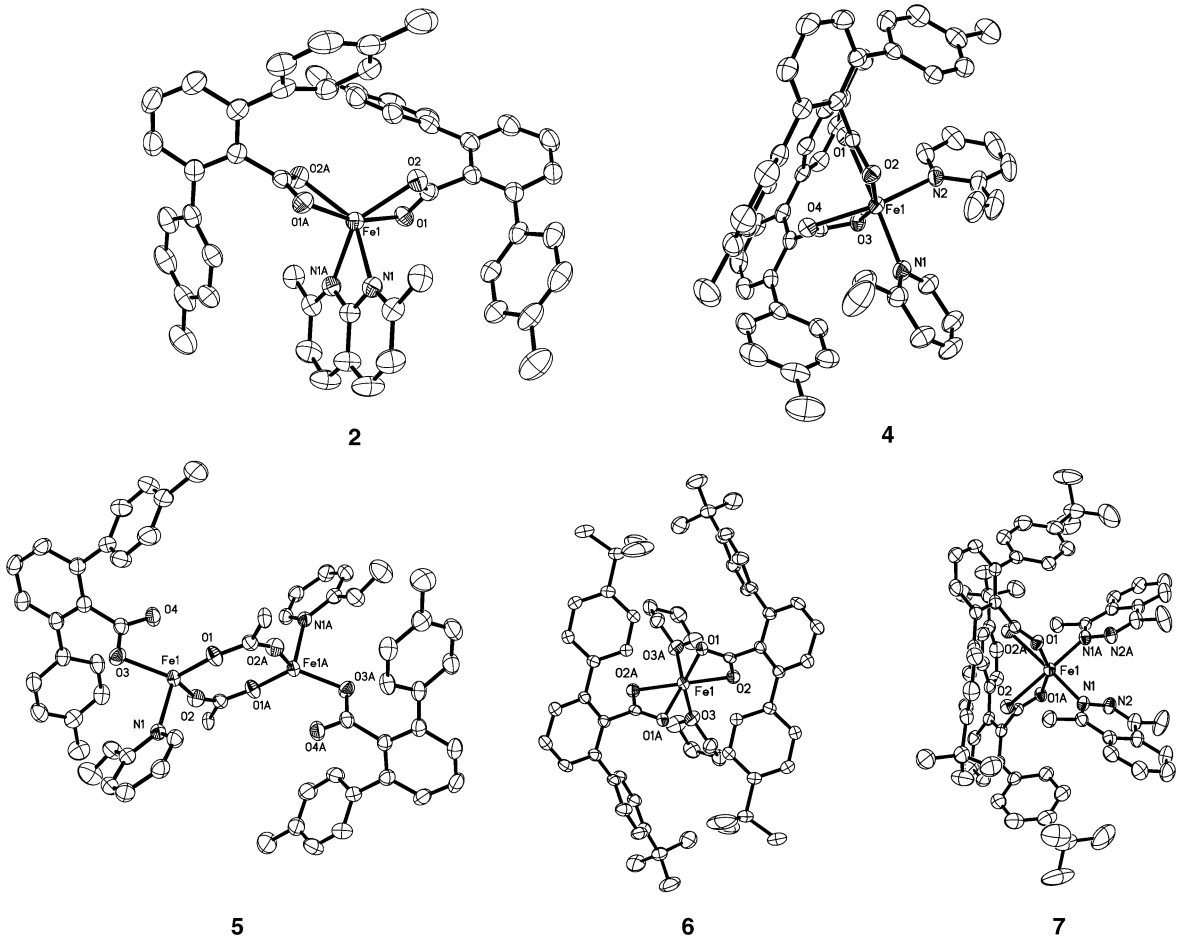


**Figure 1.** ORTEP diagrams of $[Fe(O_2CAr^{Tol})_2(Me_2\text{-napy})]$ (**2**), $[Fe(O_2CAr^{Tol})_2(vpy)_2]$ (**4**), $[Fe_2(\mu\text{-}O_2CAr^{Tol})_2(O_2CAr^{Tol})_2(vpy)_2]$ (**5**), $[Fe(O_2CAr^{4\text{-}tBuPh})_2(THF)_2]$ (**6**), and $[Fe(O_2CAr^{4-tBuPh})_2(DMP)_2]$ (**7**) showing 50% probability thermal ellipsoids for all non-hydrogen atoms (left to right, top to bottom). The phenyl rings of the bridging $Ar^{Tol}CO_2^-$ ligands in **5** are omitted for clarity.

or benzoate, attesting to the ability of the flanking phenyl groups to prevent undesired oligomerization reactions. In the absence of additional donor atoms, the 1,8-naphthyridine unit frequently adopts the chelating coordination mode evident in **2**,[64−68] whereas the bridging mode is more common when a metal−metal interaction is present to stabilize the dinuclear core,[69−75] a feature lacking in our system.

**Synthesis and Reactivity of $[Fe_2(\mu\text{-DMP})(\mu\text{-}O_2CAr^{Tol})_2(O_2CAr^{Tol})_2(THF)]$ (3). Preparation and Crystallographic Analysis of $[Fe(O_2CAr^{Tol})_2(vpy)_2]$ (4) and $[Fe_2(\mu\text{-}O_2CAr^{Tol})_2(O_2CAr^{Tol})_2(vpy)_2]$ (5).** Whereas the flexible disposition of the nitrogen lone pairs of the 1,8-naphthyridine unit permits the formation of both mononuclear and dinuclear species, the phthalazine moiety should promote dinuclearity because the lone pairs point away from one another. In support of this expectation, we note that no mononuclear compounds with $\eta^2$-bound phthalazine have been crystallographically characterized. Upon treatment of **1** with DMP, the dinuclear core remained intact, and complex **3** was isolated in excellent yield (94%). The data quality of repeated X-ray crystallographic analyses was sufficient to ascertain the gross structure of the compound, but was unsatisfactory for full complete refinement. The coordination environment of **3**, shown in Scheme 1, features two asymmetric iron sites, separated by ∼3.4 Å, that are bridged by DMP and two $Ar^{Tol}CO_2^-$ ligands. One iron is additionally coordinated by a bidentate carboxylate ligand, and a monodentate carboxylate and an additional solvent molecule complete the coordination sphere of the remaining iron center. Dinuclear compounds generally form with multidentate ligands derived from phthalazine,[76−86] but such structures are rare with phthalazine units lacking additional donor groups.[72,87−89]

Compound **3** is significant because it reproduces the syn coordination geometry of the two nitrogen donors present

(69) Døssing, A.; Larsen, S.; van Lelieveld, A.; Bruun, R. M. *Acta Chem. Scand.* **1999**, *53*, 230−234.
(70) Griffith, W. P.; Koh, T. Y.; White, A. J. P.; Williams, D. J. *Polyhedron* **1995**, *14*, 2019−2025.
(71) Munakata, M.; Maekawa, M.; Kitagawa, S.; Adachi, M. *Inorg. Chim. Acta* **1990**, *167*, 181−188.
(72) Tsuda, T.; Ohba, S.; Takahashi, M.; Ito, M. *Acta Crystallogr., Sect. C* **1989**, *C45*, 887−890.
(73) Tiripicchio, A.; Camellini, M. T.; Usón, R.; Oro, L. A.; Ciriano, M. A.; Viguri, F. *J. Chem. Soc., Dalton Trans.* **1984**, 125−131.
(74) Gatteschi, D.; Mealli, C.; Sacconi, L. *Inorg. Chem.* **1976**, *15*, 2774−2778.
(75) Gatteschi, D.; Mealli, C.; Sacconi, L. *J. Am. Chem. Soc.* **1973**, *95*, 2736−2738.
(76) Barrios, A. M.; Lippard, S. J. *Inorg. Chem.* **2001**, *40*, 1250−1255.
(77) Barrios, A. M.; Lippard, S. J. *Inorg. Chem.* **2001**, *40*, 1060−1064.
(78) Barrios, A. M.; Lippard, S. J. *J. Am. Chem. Soc.* **2000**, *122*, 9172−9177.
(79) Barrios, A. M.; Lippard, S. J. *J. Am. Chem. Soc.* **1999**, *121*, 11751−11757.

**Table 1.** Summary of X-ray Crystallographic Data for Compounds **2**, **4**, **5**·2$CH_2Cl_2$·MeOH, **6**, **7**·2THF, and **15**·3.25$CH_2Cl_2$·$Et_2O$

| | **2** | **4** | **5**·2$CH_2Cl_2$·MeOH | **6** | **7**·2THF | **15**·3.25$CH_2Cl_2$·$Et_2O$ |
|---|---|---|---|---|---|---|
| formula | $C_{52}H_{44}N_2FeO_4$ | $C_{56}H_{48}N_2FeO_4$ | $C_{101}H_{82}N_2Fe_2O_9Cl_4$ | $C_{62}H_{56}FeO_6$ | $C_{82}H_{94}N_4FeO_6$ | $C_{109.25}H_{93}N_2Fe_2SO_{14}F_3Cl_{6.5}$ |
| fw | 816.74 | 868.81 | 1721.19 | 952.92 | 1287.46 | 2089.04 |
| space group | *C*2/*c* | $P2_1/c$ | $P2_1/n$ | *C*2/*c* | *C*2/*c* | $P2_1/c$ |
| *a*, Å | 21.272(5) | 14.543(5) | 15.161(2) | 35.297(6) | 14.8112(10) | 27.237(7) |
| *b*, Å | 16.099(5) | 11.941(5) | 10.8129(16) | 11.092(2) | 31.795(2) | 14.188(4) |
| *c*, Å | 13.652(5) | 26.988(5) | 26.267(4) | 15.225(3) | 16.8180(12) | 29.326(8) |
| α, deg | | | | | | |
| *β*, deg | 114.962(5) | 103.030(5) | 93.126(3) | 114.840(3) | 104.9430(10) | 113.644(4) |
| *γ*, deg | | | | | | |
| *V*, Å$^3$ | 4239(2) | 4566(3) | 4299.7(11) | 5409.4(17) | 7652.0(9) | 10381(5) |
| *Z* | 4 | 4 | 2 | 4 | 4 | 4 |
| *T*, °C | −100 | −70 | −70 | −70 | −70 | −100 |
| $\rho_{calcd}$, g cm$^{-3}$ | 1.280 | 1.264 | 1.329 | 1.170 | 1.118 | 1.337 |
| $\mu$(Mo Kα), mm$^{-1}$ | 0.404 | 0.380 | 0.523 | 0.328 | 0.249 | 0.535 |
| *θ* range, deg | 1.99−28.28 | 1.55−28.17 | 2.04−28.26 | 1.94−28.24 | 1.28−25.00 | 1.67−25.00 |
| total data | 13206 | 27049 | 25519 | 15913 | 19849 | 75408 |
| unique data | 4885 | 10101 | 9737 | 6117 | 6730 | 18275 |
| obsd data[a] | 3598 | 8261 | 7379 | 4836 | 5466 | 14971 |
| params | 269 | 569 | 550 | 420 | 420 | 1306 |
| *R*[b] | 0.0447 | 0.0625 | 0.0609 | 0.0477 | 0.0791 | 0.0805 |
| wR$^2$ [c] | 0.1035 | 0.1281 | 0.1454 | 0.1344 | 0.2487 | 0.2048 |
| max, min peaks, e Å$^{-3}$ | 0.339, −0.234 | 0.344, −0.346 | 0.713, −0.535 | 0.431, −0.317 | 1.032, −0.542 | 1.320, −1.002 |

[a] Observation criterion: $I > 2\sigma(I)$. [b] $R = \sum||F_o| - |F_c||/\sum|F_o|$. [c] $wR^2 = \{\sum[w(F_o^2 - F_c^2)^2]/\sum[w(F_o^2)^2]\}^{1/2}$.

**Table 2.** Selected Bond Lengths (Å) and Angles (deg) for **2**, **4**, and **5**·2$CH_2Cl_2$·MeOH[a]

| bond length | | bond angle | |
|---|---|---|---|
| | | **2** | |
| Fe(1)−N(1) | 2.214(2) | N(1)−Fe(1)−N(1A) | 60.93(9) |
| Fe(1)−O(1) | 2.137(2) | N(1)−Fe(1)−O(1) | 104.86(6) |
| Fe(1)−O(2) | 2.180(2) | N(1)−Fe(1)−O(2) | 100.87(6) |
| | | O(1)−Fe(1)−O(2) | 60.83(5) |
| | | O(1)−Fe(1)−O(1A) | 161.86(8) |
| | | O(1)−Fe(1)−O(2A) | 107.90(6) |
| | | **4** | |
| Fe(1)−N(1) | 2.163(2) | N(1)−Fe(1)−N(2) | 97.84(9) |
| Fe(1)−N(2) | 2.194(2) | N(1)−Fe(1)−O(1) | 165.00(8) |
| Fe(1)−O(1) | 2.303(2) | N(1)−Fe(1)−O(2) | 105.48(8) |
| Fe(1)−O(2) | 2.065(2) | N(1)−Fe(1)−O(3) | 92.10(8) |
| Fe(1)−O(3) | 2.102(2) | N(1)−Fe(1)−O(4) | 95.16(8) |
| Fe(1)−O(4) | 2.265(2) | N(2)−Fe(1)−O(1) | 89.19(8) |
| | | N(2)−Fe(1)−O(2) | 100.68(8) |
| | | N(2)−Fe(1)−O(3) | 91.42(8) |
| | | N(2)−Fe(1)−O(4) | 149.14(8) |
| | | **5**·2$CH_2Cl_2$·MeOH | |
| Fe(1)···Fe(1A) | 4.3429(8) | O(1)−Fe(1)−O(2) | 114.46(8) |
| Fe(1)−O(1) | 2.013(2) | O(1)−Fe(1)−O(3) | 115.98(8) |
| Fe(1)−O(2) | 1.958(2) | O(1)−Fe(1)−N(1) | 97.02(8) |
| Fe(1)−O(3) | 2.030(2) | O(2)−Fe(1)−O(3) | 124.58(8) |
| Fe(1)−N(1) | 2.154(2) | O(2)−Fe(1)−N(1) | 103.08(9) |
| | | O(3)−Fe(1)−N(1) | 92.20(8) |

[a] Numbers in parentheses are estimated standard deviations of the last significant figure. Atoms are labeled as indicated in Figure 1.

**Table 3.** Selected Bond Lengths (Å) and Angles (deg) for **6**, **7**·2THF, **15**·3.25$CH_2Cl_2$·$Et_2O$[a]

| bond length | | bond angle | |
|---|---|---|---|
| | | **6** | |
| Fe(1)−O(1) | 2.250(1) | O(3)−Fe(1)−O(3A) | 95.93(8) |
| Fe(1)−O(2) | 2.118(2) | O(3)−Fe(1)−O(1) | 149.54(5) |
| Fe(1)−O(3) | 2.099(2) | O(3)−Fe(1)−O(2) | 89.81(5) |
| | | O(3)−Fe(1)−O(1A) | 92.76(6) |
| | | O(3)−Fe(1)−O(2A) | 97.22(6) |
| | | O(1)−Fe(1)−O(1A) | 94.38(7) |
| | | O(1)−Fe(1)−O(2A) | 111.98(5) |
| | | O(2)−Fe(1)−O(2A) | 169.52(7) |
| | | **7**·2THF | |
| Fe(1)−N(1) | 2.163(3) | N(1)−Fe(1)−N(1A) | 95.28(17) |
| Fe(1)−O(1) | 2.059(2) | N(1)−Fe(1)−O(1) | 101.23(11) |
| Fe(1)−O(2) | 2.384(3) | N(1)−Fe(1)−O(2) | 93.77(11) |
| | | N(1)−Fe(1)−O(1A) | 95.55(11) |
| | | N(1)−Fe(1)−O(2A) | 158.83(10) |
| | | **15**·3.25$CH_2Cl_2$·$Et_2O$ | |
| Fe(1)···Fe(2) | 3.576(1) | O(1)−Fe(1)−O(3) | 96.57(12) |
| N(1)···N(2) | 6.077(5) | O(1)−Fe(1)−O(5) | 101.03(12) |
| Fe(1)−N(1) | 2.164(3) | O(1)−Fe(1)−O(7) | 85.66(12) |
| Fe(1)−O(1) | 2.054(3) | O(1)−Fe(1)−N(1) | 160.96(13) |
| Fe(1)−O(3) | 2.017(3) | O(3)−Fe(1)−O(5) | 116.99(13) |
| Fe(1)−O(5) | 2.048(3) | O(3)−Fe(1)−O(7) | 154.85(13) |
| Fe(1)−O(7) | 2.081(3) | O(5)−Fe(1)−O(7) | 86.88(12) |
| Fe(2)−N(2) | 2.193(3) | O(7)−Fe(1)−N(1) | 82.22(13) |
| Fe(2)−O(2) | 2.084(3) | O(2)−Fe(2)−O(4) | 96.57(12) |
| Fe(2)−O(4) | 2.034(3) | O(2)−Fe(2)−O(6) | 99.44(12) |
| Fe(2)−O(6) | 1.974(3) | O(2)−Fe(2)−O(9) | 87.66(12) |
| Fe(2)−O(9) | 2.081(3) | O(2)−Fe(2)−N(2) | 167.37(12) |
| | | O(4)−Fe(2)−O(9) | 94.18(12) |
| | | O(6)−Fe(2)−O(9) | 134.94(13) |
| | | O(9)−Fe(2)−N(2) | 82.17(12) |

[a] Number in parentheses are estimated standard deviations of the last significant figure. Atoms are labeled as indicated in Figures 1 and 3.

at the active sites of sMMOH, RNR-R2, and Δ9D. To our knowledge, the only other diiron(II) compound that displays this feature in a carboxylate-rich environment is $Et_4N[Fe_2(\mu\text{-}H_2O)(\mu\text{-}O_2CCH_3)_2(O_2CCH_3)_3(C_5H_5N)_2]$.[90,91] Although this complex was formed by self-assembly, kinetic lability of the core was evident in the subsequent reaction with dioxygen to afford a ($\mu_3$-oxo)triiron(III) basic acetate complex.[90] Not surprisingly, the dinuclear core in **3** also does not remain intact upon oxidation, and preliminary reactivity studies indicate that a hexanuclear iron(III) complex forms upon exposure to dioxygen.[92]


(80) Tandon, S. S.; Thompson, L. K.; Manuel, M. E.; Bridson, J. N. *Inorg. Chem.* **1994**, *33*, 5555−5570.

(81) Chen, L.; Thompson, L. K.; Bridson, J. N. *Inorg. Chem.* **1993**, *32*, 2938−2943.

(82) Mandal, S. K.; Thompson, L. K.; Newlands, M. J.; Charland, J.-P.; Gabe, E. J. *Inorg. Chim. Acta* **1990**, *178*, 169−178.

(83) Mandal, S. K.; Woon, T. C.; Thompson, L. K.; Newlands, M. J.; Gabe, E. J. *Aust. J. Chem.* **1986**, *39*, 1007−1021.

(84) Mandal, S. K.; Thompson, L. K.; Hanson, A. W. *J. Chem. Soc., Chem. Commun.* **1985**, 1709−1711.

**Scheme 2**[a]

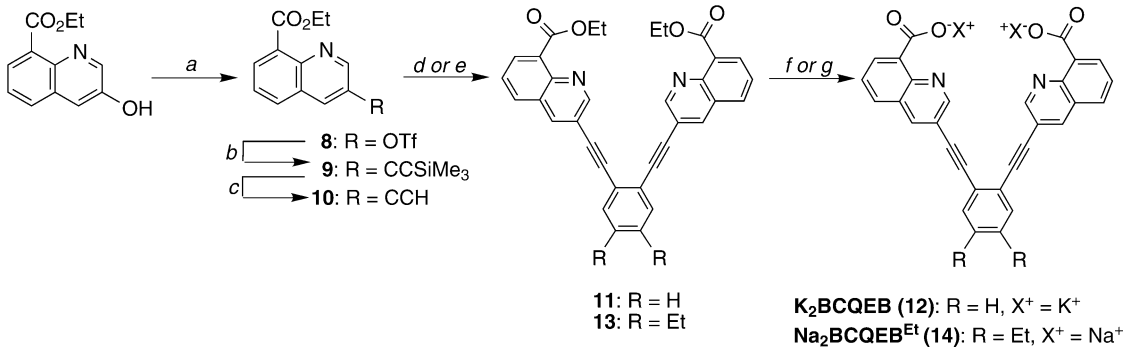


[a] (a) $Tf_2O/CH_2Cl_2$/pyridine, 95%; (b) $Me_3SiCCH/NEt_3/THF$, $[PdCl_2(PPh_3)_2]$/CuI (cat.), 80%; (c) $^nBu_4NF/THF$, 50%; (d) R = H; 1,2-diiodobenzene/$Et_2NH$, $[PdCl_2(PPh_3)_2]$/CuI (cat.), Δ, 66%; (e) R = Et; 1,2-diiodo-4,5-diethylbenzene/$Et_2NH$, $[PdCl_2(PPh_3)_2]$/CuI (cat.), Δ, 45%; (f) R = H; $KOSiMe_3$/THF; (g) R = Et; NaOH/MeOH.

The lability of the dinuclear core in **3** is further manifest by reaction with vpy to generate mononuclear **4** (Scheme 1). The pseudo-octahedral iron(II) center in this compound is ligated by two bidentate $Ar^{Tol}CO_2^-$ ligands and two vpy groups. The coordination of the carboxylate ligands is asymmetric, with Fe−O bond lengths ranging from 2.065(2) to 2.303(2) Å. The N−Fe−N bond angle of 97.84(9)° is substantially larger than that in **2**, resulting in a less distorted octahedral geometry at the iron center.

A combination of $Ar^{Tol}CO_2^-$ and vpy ligands can also support a diiron(II) core, as seen by the synthesis of **5** when **1** reacts with vpy in a ratio of 1:2 (Scheme 1). A survey of the Cambridge Structural Database revealed that **4** and **5** are the only crystallographically characterized iron compounds ligated by vpy ligands. Not surprisingly, the vpy groups in **5** are bound in an anti fashion with Fe−N bond lengths of 2.154(2) Å, and the alkene units are directed away from the metal centers. The arrangement of the four carboxylate ligands in a windmill rather than paddlewheel fashion results in an Fe···Fe separation of 4.343(1) Å that is slightly elongated relative to the intermetal distances found in related diiron compounds.[31,33,37,93] The Fe−O bond lengths of the monodentate $Ar^{Tol}CO_2^-$ ligands of 2.030(2) Å are shorter than those of the chelating carboxylates in **2** and **4**, although a weak $Fe\cdots O_{dangling}$ interaction is suggested by the ∼2.48 Å separation between Fe(1) and O(4).

**A More Sterically Demanding Carboxylate Ligand. Synthesis and Crystal Structures of $[Fe(O_2Ar^{4\text{-}tBuPh})_2(THF)_2]$ (6) and $[Fe(O_2Ar^{4\text{-}tBuPh})_2(DMP)_2]$ (7).** The propensity of the $\{Fe_2(O_2CAr^{Tol})_4\}$ core to be disrupted prompted us to modify the substituents of the *m*-terphenyl carboxylate ligands in an effort to stabilize the dimetallic unit. In order to restrict access to bimolecular reaction pathways that lead to high-nuclearity species upon oxidation, we employed the sterically demanding 4-*tert*-butyl derivative. Reaction of $Fe(OTf)_2\cdot 2MeCN$ with $NaO_2CAr^{4\text{-}tBuPh}$ in a ratio of 1:2 in THF generated mononuclear **6**, and prolonged reaction times (>12 h) did not afford a dinuclear compound. This result differs from the chemistry of diiron analogues supported by $Ar^{Tol}CO_2^-$,[31] $Ar^{4\text{-}FPh}CO_2^-$,[31] and $Ar^{Mes}CO_2^-$ ligands.[37] The stereochemistry at the iron(II) center in **6** is similar to that of **4**, with two bidentate carboxylate ligands and two THF molecules coordinating to the metal ion. The Fe−O bonds located trans to the coordinated THF molecules are elongated relative to the other bonds ($\Delta_{Fe-O}$ = 0.132(1) Å), and the $O_{THF}-Fe-O_{THF}$ bond angle of 95.93(8)° is close to the N−Fe−N angle in **4**.

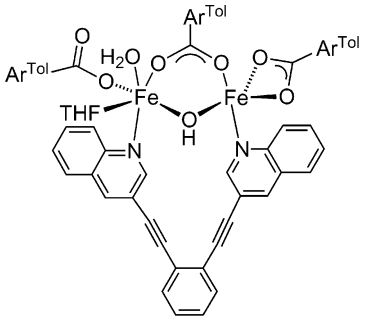


**Figure 2.** Representation of $[Fe_2(BQEB)(\mu\text{-}OH)(\mu\text{-}O_2CAr^{Tol})(O_2CAr^{Tol})_2(THF)(H_2O)]$ displaying syn nitrogen donor ligands.

Addition of either 1 or 2 equiv of DMP to **6** affords mononuclear **7** by exchange of the THF ligands, and the stereochemistry at the iron center of this compound is similar to that of **4** and **6**. One nitrogen atom of each DMP ligand remains unmetalated. Such $\eta^1$-coordination of the phthalazine unit has been observed in other compounds.[72,94−97] The *tert*-

(85) Thompson, L. K.; Hanson, A. W.; Ramaswamy, B. S. *Inorg. Chem.* **1984**, *23*, 2459−2465.
(86) Sullivan, D. A.; Palenik, G. J. *Inorg. Chem.* **1977**, *16*, 1127−1133.
(87) Whitcomb, D. R.; Rogers, R. D. *Inorg. Chim. Acta* **1997**, *256*, 263−267.
(88) Li, C.; Kanehisa, N.; Miyagi, Y.; Nakao, Y.; Takamizawa, S.; Mori, W.; Kai, Y. *Bull. Chem. Soc. Jpn.* **1997**, *70*, 2429−2436.
(89) Whitcomb, D. R.; Rogers, R. D. *J. Chem. Crystallogr.* **1995**, *25*, 137−142.
(90) Reynolds, R. A., III; Dunham, W. R.; Coucouvanis, D. *Inorg. Chem.* **1998**, *37*, 1232−1241.
(91) Coucouvanis, D.; Reynolds, R. A., III; Dunham, W. R. *J. Am. Chem. Soc.* **1995**, *117*, 7570−7571.
(92) Kuzelka, J.; Lippard, S. J. Unpublished results. Pentane vapor diffusion into an $O_2$-saturated THF solution of **3** afforded red-brown crystals of $[Fe_6(\mu_3\text{-}O)_2(\mu\text{-}OH)_6(\mu\text{-}O_2CR)_8(THF)_2]$.
(93) Lee, D.; Lippard, S. J. *J. Am. Chem. Soc.* **2001**, *123*, 4611−4612.
(94) Kettler, P. B.; Chang, Y.-D.; Chen, Q.; Zubieta, J.; Abrams, M. J.; Larsen, S. K. *Inorg. Chim. Acta* **1995**, *231*, 13−20.
(95) Abrams, M. J.; Larsen, S. K.; Shaikh, S. N.; Zubieta, J. *Inorg. Chim. Acta* **1991**, *185*, 7−15.
(96) Nicholson, T.; Zubieta, J. *Polyhedron* **1988**, *7*, 171−185.
(97) Bushnell, G. W.; Dixon, K. R. *Can. J. Chem.* **1978**, *56*, 878−883.

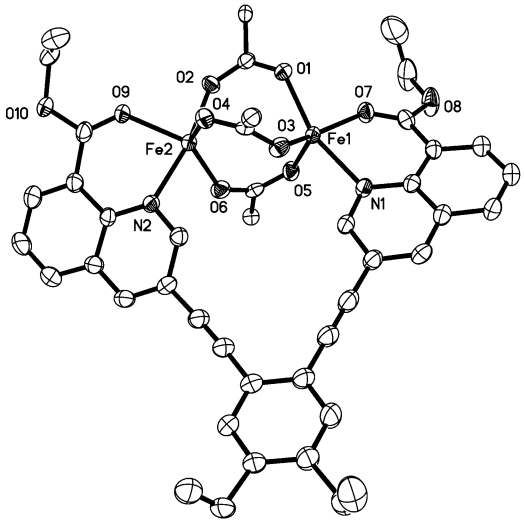


15

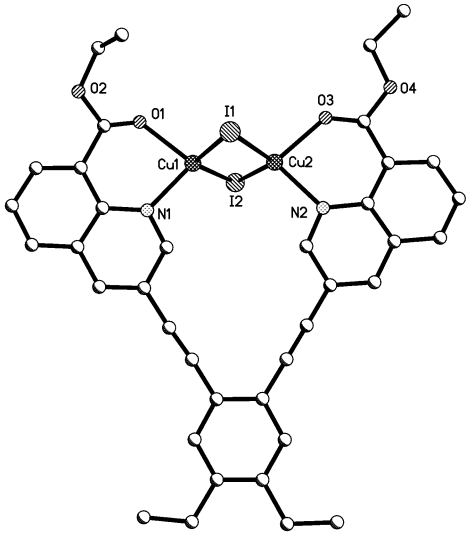


16

**Figure 3.** ORTEP diagram of the cation in $[Fe_2(Et_2BCQEB^{Et})(\mu\text{-}O_2CAr^{Tol})_3](OTf)$ (**15**) showing 50% probability thermal ellipsoids for all non-hydrogen atoms and ball-and-stick diagram showing the connectivity of $[Cu_2(Et_2BCQEB^{Et})(\mu\text{-}I)_2]$ (**16**) (left to right). The phenyl rings of the bridging $Ar^{Tol}CO_2^-$ ligands in **15** are omitted for clarity.

butyl substituents of the carboxylate ligands presumably confer too much steric bulk to permit the formation of a carboxylate-rich diiron core similar to that of **3**.

**Design and Synthesis of BCQEB Derivatives.** Studies with the ligands $Me_2$-napy and DMP illustrate the difficulty of controlling nuclearity and kinetic lability with simple units. We therefore reasoned that a ligand in which the connectivity enforces the relative disposition of the N-donors and additional donor groups promote dinuclearity should address these shortcomings. Exploratory work in our laboratory with 1,2-diethynylbenzene as a spacer between two pyridine or quinoline groups proved to be an effective strategy to enforce the desired syn coordination of two nitrogen donors, as demonstrated by the synthesis and characterization of $[Fe_2(BQEB)(\mu\text{-}OH)(\mu\text{-}O_2CAr^{Tol})(O_2CAr^{Tol})_2(THF)(H_2O)]$,[98] where BQEB is 1,2-bis(3-ethynylquinoline)benzene.[99] This complex, depicted in Figure 2, displays the desired geometry and reveals that the 1,2-diethynylbenzene spacer can support a dimetallic unit with a single atom bridge, a feature important for modeling high-valent intermediates formed in the related diiron metalloenzymes. The hydroxide-bridged diiron compound, however, could be isolated only in low yield by a synthetic route that was difficult to reproduce. Moreover, reactions with dioxygen afforded mainly oligomeric species.[98] We hypothesized that additional chelating groups should enhance the stability of the resulting diiron complex, and that incorporation of carboxylate groups into the quinoline unit would be a good strategy for producing the desired biomimetic compounds.

Scheme 2 outlines the synthesis of 1,2-bis(3-ethynyl-8-carboxylatequinoline)benzene (BCQEB) derivatives. Multigram quantities of 3-hydroxy-8-carboxylatequinoline ethyl ester were synthesized following literature procedures,[48,49] and treatment with triflic anhydride[100,101] in $CH_2Cl_2$ and pyridine yielded **8** in nearly quantitative yield. Efficient Sonogashira coupling[102] between **8** and $HCCSiMe_3$ in THF afforded **9**, the trimethylsilyl group of which was subsequently deprotected with $^nBu_4NF$ in THF to yield **10**. Compound **11** was synthesized in >65% yield by a second Sonogashira reaction, and the ethyl ester was removed by treatment with $KOSiMe_3$[103] in THF to yield the potassium salt **12**, $K_2$BCQEB. In an analogous procedure, $Et_2BCQEB^{Et}$ (**13**) was prepared by using 1,2-diiodo-4,5-diethylbenzene,[50] and ester deprotection was achieved with NaOH in MeOH affording $Na_2BCQEB^{Et}$ (**14**).

**Synthesis and Structural Characterization of $[Fe_2(Et_2BCQEB^{Et})(\mu\text{-}O_2CAr^{Tol})_3](OTf)$ (15).** Metalation of $K_2$BCQEB or $Na_2BCQEB^{Et}$ with iron(II) proved to be difficult because reaction with **1** or iron(II) salts and a variety of different carboxylate ligands invariably led to materials with poor solubility in common organic solvents, suggesting the formation of an oligomeric product. Extended structures might arise from interaction of the dangling carbonyl oxygen atom of the BCQEB scaffold and other metal ions such as Fe(II) or $K^+/Na^+$. We therefore employed as ligand $Et_2BCQEB^{Et}$, the ethyl ester of which protects one oxygen atom and precludes the formation of higher nuclearity species.

Reaction of $Fe(OTf)_2{\cdot}2MeCN$ with $Et_2BCQEB^{Et}$ and $NaO_2CAr^{Tol}$ in a ratio of 2:1:3 in THF affords compound **15** in moderate yield. As shown in Figure 3, the two iron centers adopt square pyramidal geometry and are separated by 3.576(1) Å. The diiron core is spanned by three bridging $Ar^{Tol}CO_2^-$ groups, two of which are bound in a syn, syn

(98) Farrell, J. R.; Stiles, D.; Lippard, S. J. Unpublished results.
(99) Rawat, D. S.; Benites, P. J.; Incarvito, C. D.; Rheingold, A. L.; Zaleski, J. M. *Inorg. Chem.* **2001**, *40*, 1846−1857.
(100) Subramanyam, C.; Chatterjee, S.; Mallamo, J. P. *Tetrahedron Lett.* **1996**, *37*, 459−462.
(101) Draper, T. L.; Bailey, T. R. *Synlett* **1995**, 157−158.
(102) Thorand, S.; Krause, N. *J. Org. Chem.* **1998**, *63*, 8551−8553.
(103) Laganis, E. D.; Chenard, B. L. *Tetrahedron Lett.* **1984**, *25*, 5831−5834.

fashion, whereas the third carboxylate adopts the less common syn, anti coordination mode.[104] The $Et_2BCQEB^{Et}$ ligand coordinates each metal ion through the nitrogen and carbonyl oxygen atoms of the quinolinic acid unit, forming six-membered chelate rings with O−Fe−N bite angles of 82.17(12)° and 82.22(13)°. The dinuclear core is thus stabilized, permitting a reliable synthesis of **15**. Significantly, the N-donors are bound to the iron centers in a syn fashion with Fe−N bond lengths of 2.164(3) and 2.193(3) Å. The N···N separation of 6.077(5) Å is comparable to that of the donor nitrogen atoms of the two histidine residues at the diiron(II) active sites of sMMOH (∼5 Å),[12] RNR-R2 (∼5.4 Å),[14] and Δ9D (∼6 Å).[15] The Fe−O bond lengths of the carboxylate ligands range from 1.974(3) to 2.084(3) Å, with the longer bonds located trans to the quinoline nitrogen atoms. The ester unit has Fe−O bond distances of 2.081(3) Å, which fall in the upper range of other crystallographically characterized Fe−O(C)OR units.[105−118]

**Preparation and Crystallographic Characterization of $[Cu_2(Et_2BCQEB^{Et})(\mu\text{-}I)_2]$ (16).** To probe the ability of $Et_2BCQEB^{Et}$ to support dinuclear cores displaying a range of geometries and metal−metal distances, a dicopper(I) complex was prepared. Reaction of $Et_2BCQEB^{Et}$ with 2 equiv of CuI in a mixture of $CH_2Cl_2$ and $Et_2NH$ afforded **16**. The amine solvent is necessary to dissolve CuI, and no reaction occurs in pure $CH_2Cl_2$. Although a full refinement of the crystal structure of **16** was not possible because of poor data quality, the geometry at the copper centers could be unambiguously established. In **16**, there are two pseudo-tetrahedral copper(I) centers bound to bidentate units of $Et_2BCQEB^{Et}$ and two iodide ligands. The Cu−N bond lengths, ∼2.08 Å, are shorter than the Fe−N bond distances in **15** ($\Delta_{M-N}$ ∼0.1 Å), as expected for a complex with lower coordination number. The M−O bond lengths in **16** are longer by ∼0.05 Å relative to those in **15**, however, reflecting the soft character of Cu(I) compared to Fe(II). The iodide ligands form two single atom bridges between the copper sites with Cu−I bond lengths of ∼2.59 Å. The Cu−I−Cu and I−Cu−I bond angles of ∼120° and 59°, respectively, give rise to a short Cu···Cu separation (∼2.54 Å). This distance is slightly less than the intermetal separation in metallic copper (2.56 Å), suggesting that there may be a weak copper−copper interaction. The two nitrogen atoms of $Et_2BCQEB^{Et}$ are ∼5.41 Å apart in **16**, a substantial reduction compared to that in **15** ($\Delta_{N\cdots N} > 0.6$ Å). Di($\mu$-iodo)dicopper(I) compounds supported by alkyl esters of quinaldic acid have similar geometric parameters.[119]

## Discussion

**Complexes of $Me_2$-napy and DMP.** Use of sterically hindered *m*-terphenyl-derived carboxylate ligands with the 1,8-naphthyridine and phthalazine units $Me_2$-napy and DMP afforded both mononuclear and dinuclear compounds. Complexes **2**, **4**, and **7** all feature a pseudo-octahedral iron(II) center coordinated by two carboxylates and two nitrogen donor ligands (Figure 1). Relatively long Fe−N bonds (2.163(2)−2.214(2) Å) promote bidentate, rather than monodentate, coordination of the $Ar^{Tol}CO_2^-$ and $Ar^{4\text{-}tBuPh}CO_2^-$ groups.[62,63] The carboxylate ligands in **4** and **7** are bound asymmetrically, with the Fe−O bonds located trans to the N-donors being substantially elongated (∼0.2 Å). Because of the highly distorted stereochemistry at the iron(II) center in **2**, neither of the $Ar^{Tol}CO_2^-$ ligands is bound directly opposite the $Me_2$-napy unit, and the coordination of the carboxylates is symmetric ($\Delta_{Fe-O} \sim 0.04$ Å). The coordination mode of the phthalazine moiety appears to be dictated by the nature of the ancillary ligands, binding in an $\eta^1$ fashion in **7** and in an $\eta^2$ manner in **3**. Unfavorable steric interactions arising from the large *tert*-butyl groups of $Ar^{4\text{-}tBuPh}CO_2^-$ would appear to preclude the formation of a dinuclear compound, whereas the smaller methyl substituents of $Ar^{Tol}CO_2^-$ readily support a carboxylate-rich dimetallic unit.

**Preparation of BCQEB Ligands and Metal Complexes.** The BCQEB ligands were designed and synthesized to enforce dinuclearity and kinetic stability on the diiron(II) unit, features that were difficult to maintain with $Me_2$-napy and DMP. Compound **8** serves as a convenient starting material, and a series of Sonogashira coupling reactions afforded the BCQEB derivatives in three to four synthetic steps (Scheme 2). The connectivity of the molecular scaffold ensures that the separation of nitrogen atoms remains close to that observed for the N-donors of the histidine residues in sMMOH, RNR-R2, and Δ9D (∼5−6 Å),[12,14,15] and incorporation of a chelating moiety, ester or carboxylate, is an effective strategy for promoting dinuclearity upon metalation. The syntheses of compounds with well-defined dimetallic cores were effected with the ligand $Et_2BCQEB^{Et}$, affording $[Fe_2(Et_2BCQEB^{Et})(\mu\text{-}O_2CAr^{Tol})_3](OTf)$ (**15**) and $[Cu_2(Et_2BCQEB^{Et})(\mu\text{-}I)_2]$ (**16**), illustrated in Figure 3.

**Utilization of BCQEB-Derived Ligands and Relevance to High-Valent Intermediates in Non-Heme Diiron En-**

(104) Rardin, R. L.; Tolman, W. B.; Lippard, S. J. *New J. Chem.* **1991**, *15*, 417−430.
(105) Schobert, R. *J. Organomet. Chem.* **2001**, *617*−*618*, 346−359.
(106) Doherty, S.; Hogarth, G.; Waugh, M.; Scanlan, T. H.; Elsegood, M. R. J.; Clegg, W. *J. Organomet. Chem.* **2001**, *620*, 150−164.
(107) Kongsaeree, P.; Tanboriphan, S.; Tarnchompoo, B.; Thebtaranonth, Y. *Acta Crystallogr.* **1999**, *C55*, 2007−2010.
(108) Schobert, R.; Pfab, H.; Mangold, A.; Hampel, F. *Inorg. Chim. Acta* **1999**, *291*, 91−100.
(109) Kandler, H.; Bidell, W.; Jänicke, M.; Knickmeier, M.; Veghini, D.; Berke, H. *Organometallics* **1998**, *17*, 960−971.
(110) Doherty, S.; Elsegood, M. R. J.; Clegg, W.; Mampe, D. *Organometallics* **1997**, *16*, 1186−1192.
(111) Akita, M.; Terada, M.; Moro-oka, Y. *Chem. Commun.* **1997**, 265−266.
(112) Almeida, S. S. P.; Duarte, M. T.; Ribeiro, L. M. D.; Gormley, F.; Galvão, A. M.; Fraústo da Silva, J. J. R.; Pombeiro, A. J. L. *J. Organomet. Chem.* **1996**, *524*, 63−66.
(113) Szafert, S.; Lis, T.; Drabent, K.; Sobota, P. *J. Chem. Crystallogr.* **1994**, *24*, 197−202.
(114) Görls, H.; Jäger, E.-G. *Cryst. Res. Technol.* **1991**, *26*, 349−355.
(115) Akita, M.; Terada, M.; Oyama, S.; Sugimoto, S.; Moro-oka, Y. *Organometallics* **1991**, *10*, 1561−1568.
(116) Montlo, D.; Suades, J.; Dahan, F.; Mathieu, R. *Organometallics* **1990**, *9*, 2933−2937.
(117) Mitsudo, T.; Watanabe, H.; Watanabe, K.; Watanabe, Y.; Kafuku, K.; Nakatsu, K. *Organometallics* **1982**, *1*, 612−618.
(118) Bonnet, J. J.; Mathieu, R.; Ibers, J. A. *Inorg. Chem.* **1980**, *19*, 2448−2453.
(119) Tompkins, J. A.; Maxwell, J. L.; Holt, E. M. *Inorg. Chim. Acta* **1987**, *127*, 1−7.

**zymes.** A comparison of structures **15** and **16** allows the efficacy of the BCQEB framework to facilitate modeling of non-heme diiron enzymes to be evaluated. The ligand $Et_2BCQEB^{Et}$ supports both four- and five-coordinate complexes, and accommodates either three $\mu$-1,3-carboxylate ligands (**15**) or two single-atom bridging groups (**16**). The structural flexibility of the ligand scaffold is manifest in the range of metal−metal and N···N distances, ∼1 and 0.6 Å, respectively, supported by $Et_2BCQEB^{Et}$. Significantly, the syn disposition of the nitrogen donors is enforced with this ligand, which thus mimics histidine residues supplied by the four-helix bundle surrounding the diiron active sites of sMMOH, RNR-R2, and Δ9D. The geometry of catalytically active species in these non-heme diiron enzymes differs substantially from their reduced and oxidized forms, and the ability of a ligand to support such variety of the dinuclear core structure is crucial for the preparation of functional model analogues. The flexibility of $Et_2BCQEB^{Et}$ satisfies this requirement, thus representing a significant achievement toward the goal. Moreover, compound **16** accommodates the short metal−metal separation in the $\{M_2O_2\}$ core of intermediate Q in MMOH. The ability of the BCQEB framework to support such a structure indicates its suitability for modeling biologically relevant dimetallic species.

## Summary and Conclusions

The ligands $Me_2$-napy and DMP were introduced in an attempt to model the syn coordination of the two histidine residues at the diiron cores of sMMOH, RNR-R2, and Δ9D. In the absence of additional donor groups, the 1,8-naphthyridine and phthalazine fragments yielded iron(II) compounds, the nuclearity and kinetic stability of which were difficult to control. To address these challenges, the BCQEB-derived ligands were prepared and employed in the synthesis of $[Fe_2(Et_2BCQEB^{Et})(\mu\text{-}O_2CAr^{Tol})_3](OTf)$ (**15**) and $[Cu_2(Et_2BCQEB^{Et})(\mu\text{-}I)_2]$ (**16**). Both **15** and **16** feature dinuclear cores in which the desired syn disposition of nitrogen donors is enforced, and the range of M···M and N···N distances observed in these compounds attests to the structural flexibility of the BCQEB framework. The synthesis and diiron(II) complexes of other BCQEB derivatives and exploration of their oxidation chemistry are currently under investigation.

**Acknowledgment.** This work was funded by grants from the National Science Foundation and National Institute of General Medical Sciences. J.K. acknowledges NSERC for a graduate student fellowship. J.R.F. was an NIH postdoctoral fellow. We thank Dylan Stiles for assistance in preparing the first diethynylbenzene ligands and complexes investigated in our laboratory, Ms. Li Li of the MIT Department of Chemistry Instrumentation Facility for collecting the ESI-MS spectra, and Prof. M.-H. Baik for helpful discussion.

**Supporting Information Available:** FT-IR data for compounds **2**−**16**, the full numbering schemes of compounds **2**, **4**−**7**, **15**, and **16**, and corresponding X-ray crystallographic files in CIF format. This material is available free of charge via the Internet at http://pubs.acs.org.

IC034928E